Supplementary material

(Dated: 19 January 2024)

TABLE I. Recording parameters for each experiment: The recording mode – single-frame (sf) or double-frame (df), the time increment between two consecutive frames used in the PIV analysis, Δt (s)

	recording mode	Δt
S1	sf	2.500
S2	sf	1.333
S3	sf	0.667
S4	sf	0.200
S5	sf	0.133
W1	sf	0.067
W2	df	5.000×10^{-4}
W3	df	3.500×10^{-4}
W4	df	3.500×10^{-4}

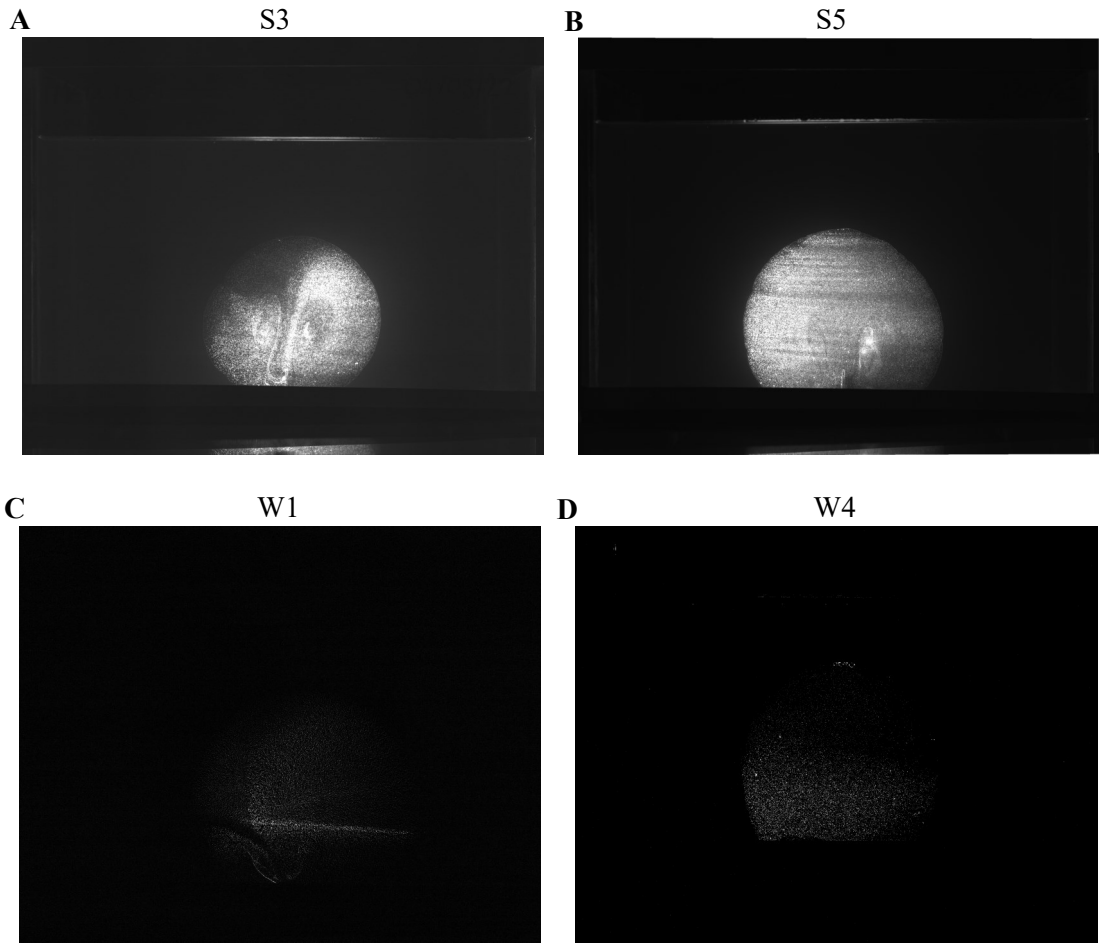

FIG. 1. Raw camera images showing fluorescent particles at a snapshot in time during fracture propagation, for experiment A) S3 (Multimedia Available Online) , B) S5 (Multimedia Available Online), C) W1 (Multimedia Available Online), D) W4 (Multimedia Available Online).

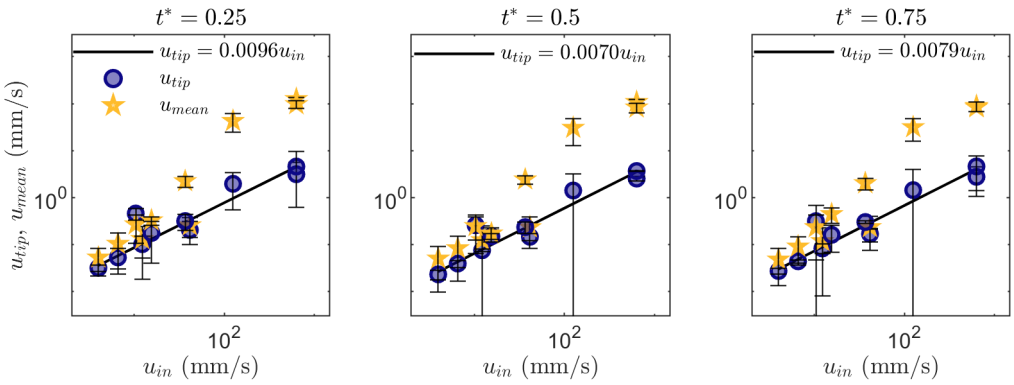

FIG. 2. Vertical tip velocities u_{tip} (blue circles) and mean flow velocities u_{mean} (yellow stars) plotted against the injection velocity u_{in}, at dimensionless times of 0.25, 0.5 and 0.75. The line of best fit between u_{tip} and u_{in} is shown for all experiments excluding S4.

TABLE II. Relevant parameters for assessing the suitability of the tracer particles in the PIV analysis: flow timescale, Δt (s), Stokes particle relaxation time, $\tau_r = \frac{d_p^2 \rho_p}{18\mu}$ (s), fluid jet velocity u_{tip} (mm/s), fluid jet velocity u_{jet} (mm/s), magnitude of representative downwards flow velocity $|u_{down}|$ (mm/s), Stokes particle velocity $U_g = \frac{d_p^2(\rho_p - \rho)g}{18\mu}$ (mm/s), Stokes number, $St = \tau_r u_{jet}/d_p$.

	Δt	τ_r	u_{tip}	u_{jet}	$\lvert u_{down}\rvert$	U_g	St
S1	2.500	3.67×10^{-7}	0.023	0.375	0.053	0.001	2.79×10^{-6}
S2	1.333	3.67×10^{-7}	0.040	0.683	0.088	0.001	5.04×10^{-6}
S3	0.667	3.67×10^{-7}	0.076	1.229	0.119	0.001	9.03×10^{-6}
S4	0.200	3.67×10^{-7}	0.258	1.925	0.183	0.001	1.41×10^{-5}
S5	0.133	3.67×10^{-7}	0.147	1.591	0.106	0.001	1.17×10^{-5}
W1	0.067	1.65×10^{-4}	0.236	6.907	2.573	0.262	0.023
W2	5.00×10^{-4}	1.65×10^{-4}	58.565	138.999	58.565	0.262	0.448
W3	3.50×10^{-4}	1.65×10^{-4}	153.974	202.533	153.974	0.262	0.700
W4	3.50×10^{-4}	1.65×10^{-4}	124.827	224.240	124.827	0.262	0.780

I. TRACER PARTICLES

The tracer particles in PIV analysis should be passively carried with fluid streamlines, with the particle relaxation time τ_R smaller than the smallest flow timescale (here assumed to be Δt). For tracer particle errors to be $< 1\%$, the Stokes number St – the ratio of the characteristic time scales of a particle in a flow and the flow itself[1] – should be < 0.1. Furthermore, the Stokes settling velocity U_g should be smaller than the characteristic flow velocities[2]. These conditions are achieved in all experiments (Tab. II).

II. REFRACTIVE INDEX OF MATERIALS

The refractive index (RI) of a material represents the refractive angle of light as it passes through, which changes at the interface between two materials with mismatching RI values. When applying PIV to multiphase flows, RI differences can lead to distortions and blurriness of tracer particles[3]. Buoyant jet experiments have shown that mismatching RI values between the jet and ambient fluid results in over-prediction of fluctuating turbulent effects in the jet, yet the effect on

errors in mean flow measurements is less significant[3]. In laminar flows with very small fluctuations from the mean velocity, planar PIV can therefore provide reasonable estimates of the 2D mean flow profiles through an RI-mismatched interface.

The RIs of the solid gelatine and liquid silicone oil were measured for several different samples using an Eclipse hand held refractometer. The RI of solid gelatine was measured at different temperatures and for several different samples. At 2.5 wt %, the RI was consistently measured as approximately 1.33586. Note that the RI of a material changes with temperature, yet any changes within our experimental temperature range were beyond the precision of the refractometer. The RI difference between water and gelatine is approximately 0.002, which has been considered an acceptable level of error in previous work[4,5]. The *RI* mismatch between silicone oil and gelatine is much more significant at 0.072. However, the silicone oil experiments are all laminar due to the high fluid viscosity. Although some blurriness can be seen in the raw camera images, the PIV method was able to compute reliable vectors with high correlation values. A qualitative inspection of the flow recording also clearly shows the observed flow pattern provided by the PIV data (Fig. 1A,B, multimedia view).

III. MEASURING FRACTURE THICKNESS

Two experiments – WH and SH – were conducted to approximate the fracture thickness of low viscosity (water) and high viscosity (silicone oil) injections (Fig. 5, multimedia view). Experiment WH was conducted in the same tank of gelatine as experiment W3, where seeded water was injected into a second injection port 10 cm away from the central port. The tank was rotated so that the camera recorded the $y-z$ plane of fracture growth, where the contrast between the seeded fluid and non-seeded gelatine allowed for b approximations within DaVis. In experiment SH, the gelatine host was seeded instead, and injected with non-seeded silicone oil.

To create seeded gelatine the tracer particles were added to cold water in the experimental tank before hot liquid gelatine was added. The mixture was then continuously stirred to distribute the particles, and the tank was put in the refrigerator once the mixture had reached a temperature of approximately 22 degrees – the temperature at which solidification starts to occur. It was important that the particles did not fall out of suspension before solidification. To reach this cool temperature, a higher proportion of cold to hot water was used.

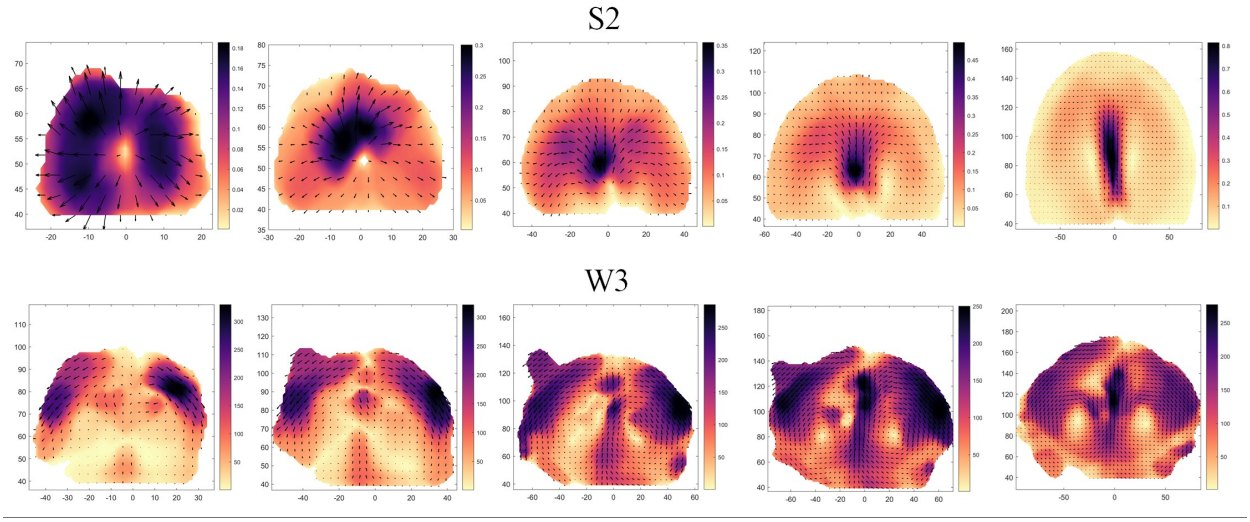

FIG. 3. Flow vectors and contours of velocity magnitude (mm/s), showing the development of the steady flow structure in the initial stages of fracture propagation. Each vector is shown to scale, and every third vector is plotted.

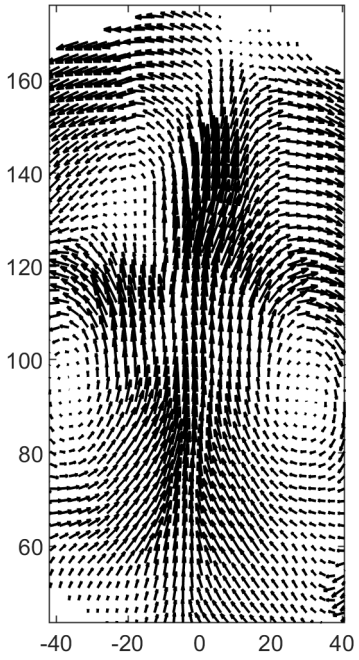

FIG. 4. A closer look at the velocity vectors in the central jet for experiment W3. The uniform vectors suggest that the jet is stable and laminar.

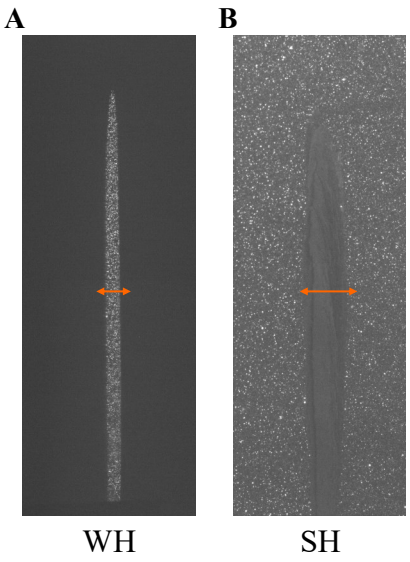

FIG. 5. Images used to approximate the fracture thickness of A) the low-viscosity water experiments (using WH), and B) the high-viscosity silicone oil experiments (SH). The images show the fracture in the $y-z$ plane. (multimedia view)

REFERENCES

[1]C. Tropea, A. L. Yarin, J. F. Foss, *et al.*, *Springer handbook of experimental fluid mechanics*, Vol. 1 (Springer, 2007).

[2]C. E. Brennen, "Fundamentals of multiphase flow," (2005).

[3]H. Mishra and J. Philip, "Importance of refractive index matching of fluids for PIV and PLIF measurements in buoyant jets," in *Proceedings of 16th Asian Congress of Fluid Mechanics* (Springer, 2021) pp. 277–284.

[4]J. L. Kavanagh, A. J. Burns, S. Hilmi Hazim, E. P. Wood, S. A. Martin, S. Hignett, and D. J. Dennis, "Challenging dyke ascent models using novel laboratory experiments: Implications for reinterpreting evidence of magma ascent and volcanism," Journal of Volcanology and Geothermal Research **354**, 87–101 (2018).

[5]S. Pansino, A. Emadzadeh, and B. Taisne, "Magma Flow Patterns in Dikes: Observations From Analogue Experiments," Journal of Geophysical Research: Solid Earth **128** (2023), 10.1029/2022jb025463.